

## CWRF Ready for Climate Service

Xin-Zhong Liang<sup>1</sup> and Julian X.L. Wang<sup>2</sup>

<sup>1</sup>Earth System Science Interdisciplinary Center, University of Maryland, College Park, MD

<sup>2</sup>NOAA Air Resources Laboratory, Silver Spring, MD

The CWRF has been developed as the Climate *extension* of the Weather Research and Forecasting model (WRF, Skamarock *et al.* 2008) by incorporating numerous improvements in representation of physical processes and integration of external (top, surface, lateral) forcings that are crucial to climate scales, including interactions between land–atmosphere–ocean, convection–microphysics and cloud–aerosol–radiation, and system consistency throughout all process modules (Liang *et al.* 2011). This extension inherits all WRF functionalities for numerical weather prediction while enhancing the capability for climate modeling. As such, it can be applied for seamless weather forecast and climate prediction. The CWRF has been built with an unprecedentedly comprehensive *ensemble* of alternative parameterization schemes for each of the key physical processes, including surface (land, ocean), planetary boundary layer, cumulus (deep, shallow), microphysics, cloud, aerosol, and radiation, and their interactions. This facilitates the use of an optimized physics ensemble approach to improve weather or climate prediction along with a reliable uncertainty estimate. The CWRF also emphasizes the societal *service* capability to provide credible information for climate impacts analyses. For that, it has been coupled with detailed models of terrestrial hydrology, coastal ocean, crop growth, air quality, and recently expanding interactive water quality and ecosystem. Their outputs will form a scientific basis for decision makers to select optimal pathways to achieve economic, societal and environmental goals.

The CWRF improvements have been accomplished through iterative, extensive model refinements, sensitivity experiments, and rigorous evaluations over the past 9 years under close collaborations between the Illinois State Water Survey in the University of Illinois at Urbana-Champaign (2003-2010), the Earth System Science Interdisciplinary Center (ESSIC) in the University of Maryland at College Park (2011 onward), the NOAA Air Resource Laboratory (ARL), and the NOAA Center for Atmospheric Sciences (NCAS). As a result, the CWRF has demonstrated greater capability and better performance in simulating the U.S. regional climate than the existing CMM5 (Liang *et al.* 2004b) and the original WRF. The present study provides an introduction of the CWRF for its application over the U.S., elaborating a few unique features that are relevant to providing credible model results for climate service.

### CWRF physical process representations

Figure 1 illustrates the current CWRF physics options and executing structure (see all the abbreviations and acronyms listed after the References). There are seven major drivers that each controls multiple alternative schemes for the physical processes of cloud, aerosol, radiation, surface, PBL, cumulus, and microphysics, in the sequential order of computation. The first three drivers (*cloud, aerosol, radiation*) form the Cloud-Aerosol-Radiation (CAR) ensemble modeling system that incorporates over 10<sup>18</sup> different ways to simulate interactions among cloud, aerosol and radiation, developed from seven packages available in the leading global and regional models around the world. This replaces the original WRF single *radiation* driver that consists of the CAM and AER packages, and the MISC schemes now obsolete. The *surface* driver manages all schemes handling surface and subsurface processes over land and oceans, as well as surface-atmosphere flux exchanges. In particular, the CWRF adds the advanced CSSP and CROP for terrestrial hydrology and crop growth over land, and SOM and UOM for mixed-layer and upper ocean effects. The two urban schemes are separated from the NOAA and now work with all land surface schemes. All 7 surface layer schemes, originally tied to specific options, are now interchangeable for all *surface* and *PBL* schemes. The *PBL* driver hosts 7 WRF plus 2 new (CAM, UW) PBL schemes, all of which are integrated with the ORO

module accounting for orographic turbulence stress and gravity-wave drag. The *cumulus* driver provides the hub for 7 WRF plus 6 new (GR, ZML, CSU, GFDL, MIT, ECP) deep cumulus schemes, all of which are conjunctive with a shallow convection scheme (UW). A consistent switch is added to control whether shallow convection is activated internally in 8 deep cumulus schemes or done externally by the UW scheme. The *microphysics* driver harnesses 11 microphysics schemes of the WRF.

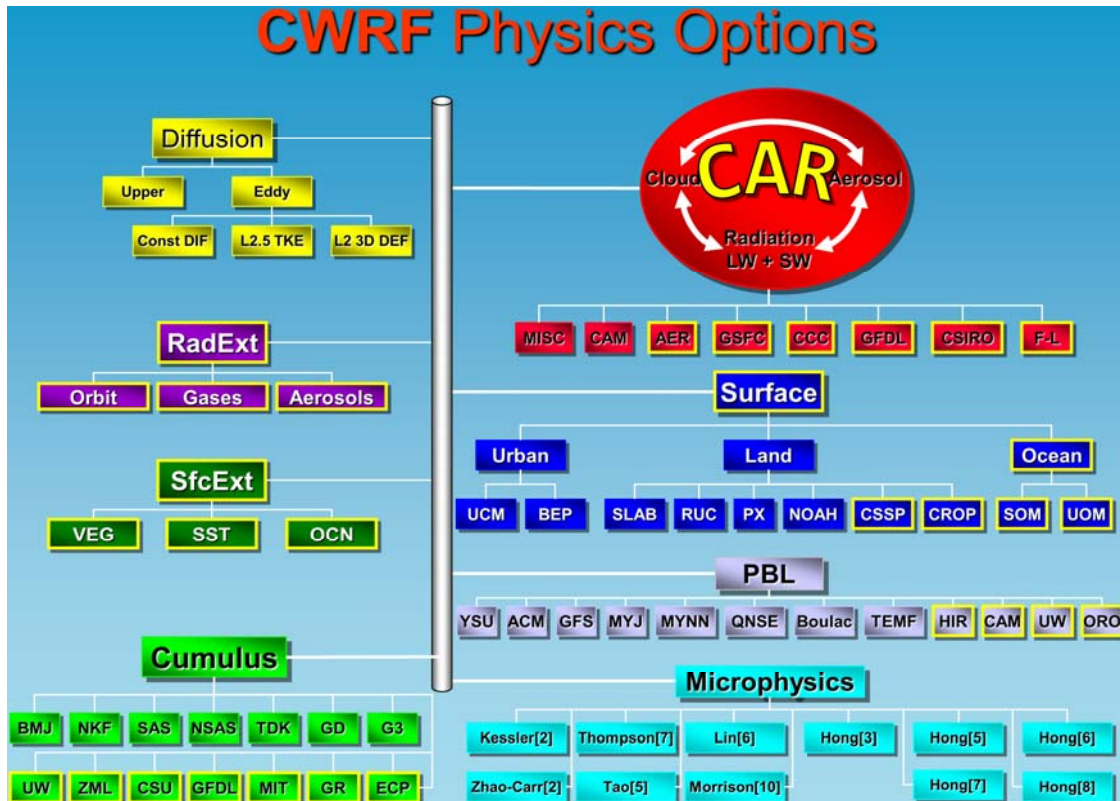


**Fig. 1** The schematic of the current CWRF physics options and executing sequence from the top down. The CAR ensemble system and all modules or schemes outlined in yellow are additions specifically developed for the CWRF, while others are inherited from the WRF.

Importantly, we strove to make all alternative schemes in the CWRF fully coupled across all drivers with plug-and-play interfaces. Even without counting the grand CAR ensemble, the CWRF currently contains over  $10^6$  configurations modeling the surface, PBL, cumulus, and microphysics processes and their interactions. To achieve this, substantial efforts have been made to scrutinize all individual schemes for consistency and incorporate suitable algorithms for missing variables to enable the overall system coupling. Particular care has been taken to ensure continuous model integration that can be restarted at any interval while resulting in bit-by-bit agreement. This is not trivial, especially if time intervals differ among executing individual physics drivers. A seamless averaging procedure is implemented to replace cumulative variables, while pertaining to model prediction, by their averages between two consecutive steps of the driver at work. This is especially effective for precipitation fields (convective/resolved rainfall/snowfall) that are used for different purposes in the *cumulus*, *microphysics*, *surface*, *cloud*, and *aerosol* drivers. Other cumulative variables for diagnostic outputs, such as surface water and energy budget fields, can be set to zero at any restart check point to reduce truncation errors. As such, the CWRF can be run safely for a long-term climate simulation with frequent restarts as needed and with varying time steps for all 7 physics drivers. On the other hand, the WRF<sup>1</sup> with

<sup>1</sup> Note that the WRF can be configured to many versions using different combinations of physics schemes. The reported WRF configurations are limited. The statement was drawn upon our own experience with the WRF runs and through review of several journal manuscripts of others.

several tested configurations has been reported to result in numerical instability or serious drift that are prohibitive for continuous climate simulations.

### CWRF advanced terrestrial hydrology prediction

The CWRF incorporates a Conjunctive Surface-Subsurface Process model (CSSP) to predict soil temperature/moisture distributions, terrestrial hydrology variations, and land-atmosphere flux exchanges. The CSSP is rooted in the Common Land Model (CoLM; Dai *et al.* 2003, 2004) with a few updates from the Community Land Model version 3.5 (CLM3.5; Oleson *et al.* 2008). It is built upon realistic distributions of surface (soil and vegetation) characteristics (Liang *et al.* 2005a,b), and with significant improvements in representing surface energy and hydrology processes. These include an improved dynamic-statistical parameterization of land surface albedo (Liang *et al.* 2005c); a 3-D subsurface hydrologic model with a scalable representation of subgrid topographic control on soil moisture (Choi *et al.* 2007); an explicit treatment of surface-subsurface flow interaction (Choi 2006; Choi and Liang 2010; Choi *et al.* 2011); an unconfined aquifer below the bedrock (Yuan and Liang 2011a). The CSSP integrates vertical water exchange (precipitation, evaporation, transpiration, infiltration) and horizontal water movement (across grids) to predict surface and subsurface runoff resulting from rainfall excess, saturation depletion and lateral flows due to resolved and subgrid topographic controls.

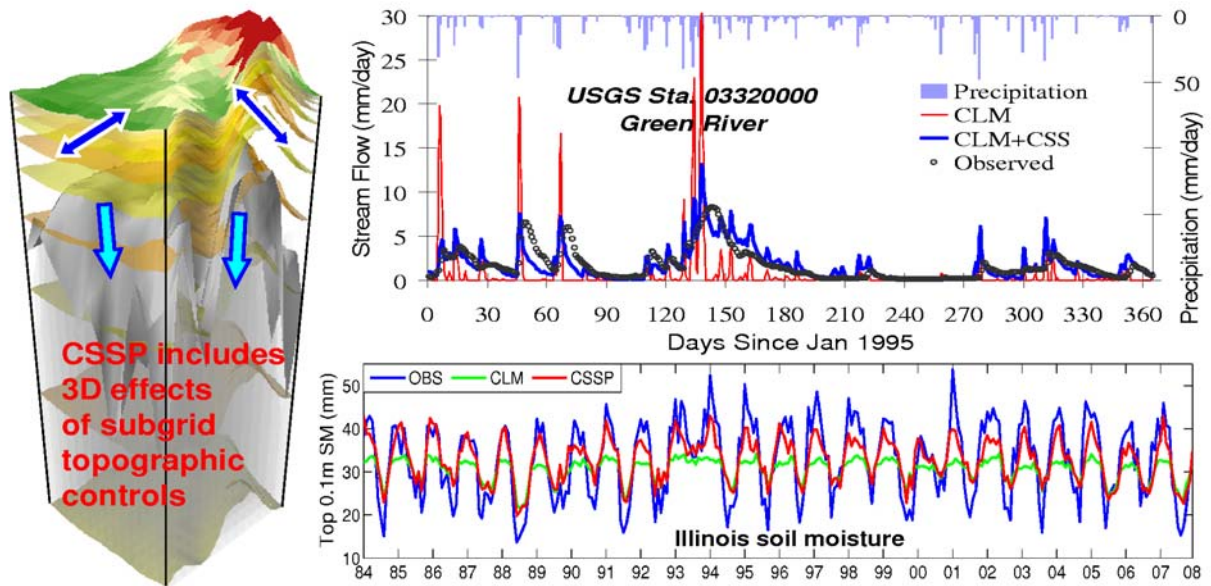


**Fig. 2** The CSSP improves terrestrial hydrology prediction over the CLM. This includes incorporation of 3D effects of subgrid topographic controls (*left*), depiction of realistic streamflow variations over major watersheds (*right top*), and capture of seasonal-interannual variations of soil moisture observed in Illinois (*right bottom*).

A comprehensive evaluation against observations at regional-local scales over the contiguous U.S. has demonstrated that the CSSP overall performance is superior to both the CoLM and CLM3.5 (Yuan and Liang 2011a). A recent comparison of offline integrations driven by observational reanalysis data also revealed that the CSSP has clear advantages in modeling the U.S. terrestrial hydrology (soil moisture, runoff) over the NOAA used in the NCEP CFS. As a result, the CWRF using the CSSP generates not only more realistic phase (higher correlations) but also better amplitude (deviation ratios closer to 1) of the soil moisture seasonal-interannual variations throughout the root zone than the WRF using the NOAA (Liang *et al.* 2011). Figure 2 depicts an example CSSP improvement over its origin CLM, which produces streamflow pulse fluctuations as a result of quick response to rainfall events, causing no recession time, overall runoff underestimation, and weak seasonal-interannual soil moisture variability. This advance in representing the terrestrial hydrology by the CSSP over NOAA has other major climate benefits.

### CWRF physics ensemble skill enhancement

The CWRF incorporates a massive suite of alternative numerical schemes for microphysics, convection, cloud, aerosol, radiation, surface, turbulence and transport processes, all of which are fully coupled with nonlinear interactions to ultimately determine its climate prediction. No single scheme can capture all aspects of the observed climate, but produce predictive skill dependent of climate regimes (Liang *et al.* 2004a,b; Mapes *et al.* 2004). Consensus prediction based on the ensemble of multiple models or multiple physics configurations of a model may offer significant skill enhancement (Krishnamurti *et al.* 1999; Peng *et al.* 2002; Palmer *et al.* 2004; Liang *et al.* 2007; Wang *et al.* 2009).

Here we tested an extremely limited subset of the CWRF full ensemble, focusing on the control configuration and all major alternative schemes across each physics driver, altered one at a time. In total, there are 26 CWRF simulations. Each simulation is driven by the NCEP Reanalysis-2 LBCs and integrated from 1 November 1992 to 31 December 1993. During the summer of that year, record flooding occurred in the Mississippi River basin. Figure 3 illustrates spatial frequency distributions of pointwise correlation coefficients and root-mean-square errors (*RMSE*) of daily mean rainfall variations between observations and all CWRF simulations. Shown are also the ensemble results as the averages of all runs with equal or optimal weights. The optimal weight results from local *RMSE* minimization, and the skill score depicts the upper limit of daily rainfall predictability that can be achieved from the best optimization of the ensemble. Clearly, the ensemble average of the alternative physics configurations using an equal weight substantially increases the predictive skill over all individuals, with more frequent occurrences of higher correlation coefficients and smaller *RMSE*. The improvement by the ensemble is realized because distinct regions are identified where each configuration complementarily captures certain but not all observed signals. The skill enhancement is most pronounced in summer, followed by autumn and spring, whereas rather weak in winter (Liang *et al.* 2011). Note that the ensemble average using the localized optimal weights has predictive skill significantly higher than that using the equal weight as well as the individuals throughout the entire year. Thus, there exists substantial room to further enhance that skill through intelligent optimization.

### CWRF downscaling improvement to CFS climate prediction

We have recently demonstrated that the mesoscale CWRF downscaling produces significant skill enhancement to the driving NCEP CFS seasonal forecast for winter precipitation during 1982-2008 (Yuan and Liang 2011b). Figure 4a compares spatial frequency distributions of *RMSE* of seasonal mean precipitation interannual variations predicted by the CFS and downscaled by the CWRF. The statistics are based on all land grids over the entire inner domain (U.S., southern Canada, and northern Mexico) from 5 realizations. All CWRF results consistently reduce CFS forecast errors. The reduction is obvious at all

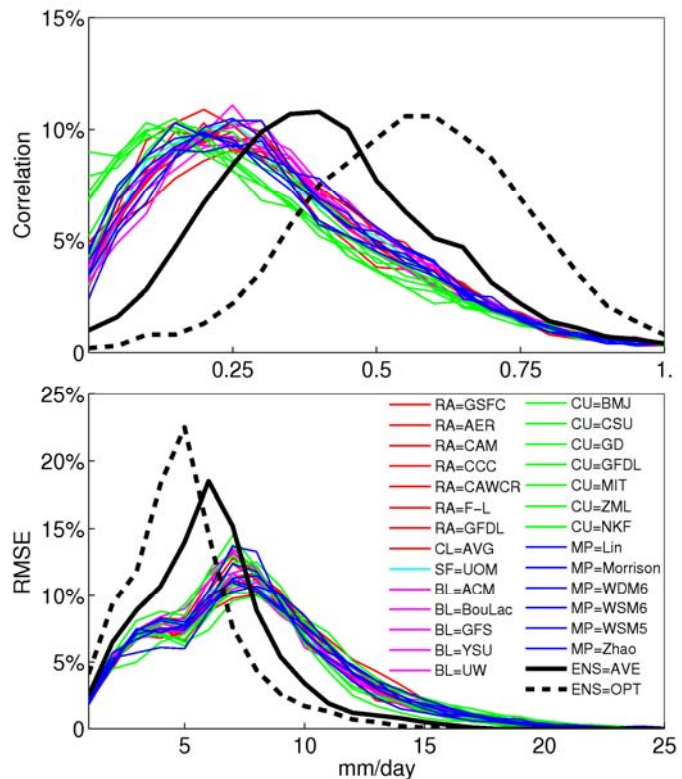


**Fig. 3** Spatial frequency distributions of correlations (top) and rms errors (bottom) between CWRF and observed daily mean rainfall variations in summer 1993. Each line depicts a specific configuration in group of the five key physical processes (color). The ensemble result (ENS) is the average of all runs with equal (Ave) or optimal (OPT) weights, shown as black solid or dashed line.

forecast lead times, with the *RMSE* peaks decreased by about 0.5 mm/day. Figure 4b illustrates the CWRP minus CFS differences in equitable threat score (*ETS*) of seasonal mean precipitation forecasts. The CFS forecast skill decreases rapidly for heavy rainfall events, while the CWRP maintains a good level across the range. On average, the CWRP reduces CFS forecast *RMSE* by 22%, increases *ETS* by 0.08-0.15, and produces greater skill for heavy rainfall events.

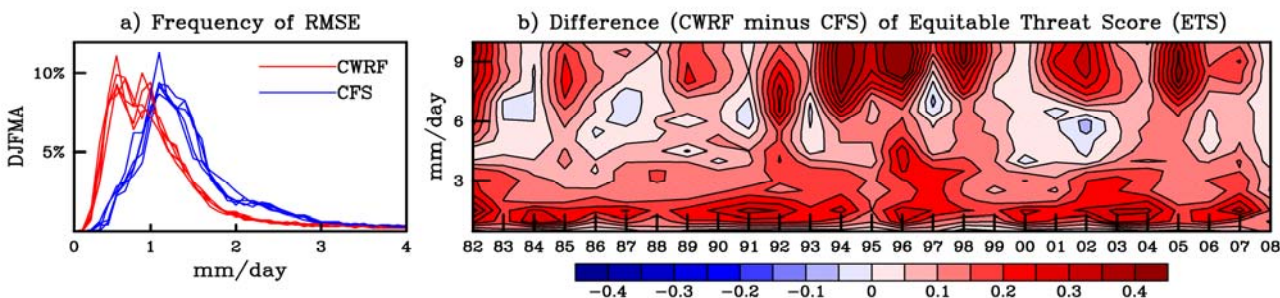


**Fig. 4** a) Spatial frequency distributions of *RMSE* (mm/day) predicted by the CFS and downscaled by the CWRP and b) CWRP minus CFS differences in *ETS* for seasonal mean precipitation interannual variations. The statistics are based on all land grids over the entire inner domain for DJFMA from the 5 realizations during 1982-2008.

Note that the *ETS* differences are larger in ENSO-neutral years than in strong anomalous years. For instance, smaller enhancements are identified in years with La Niña (1984, 1988) and El Niño (1986, 1991, 2002). During these abnormal years, significant ENSO signals presented in the planetary circulation, and thereby the CFS has higher seasonal climate predictability, especially for wintertime when global anomalies are more intense. As a result, the advantage of the CWRP downscaling over the CFS forecast is relatively weaker than ENSO-neutral years. A further analysis (not shown) indicates that the CWRP simulates more accurate number of rainy days than the CFS over the northern and western U.S. due to the refined representation of orographic effect, shallow convection, and terrestrial hydrology, and also more realistically captures the broad region of extreme rainfall over the Gulf States and maximum dry spell length along the Great Plains, as well as their contrasts between El Niño and La Niña events. In conclusion, the CWRP downscaling exhibits significant advantages for regional precipitation prediction, especially during years with weak planetary anomalies.

### CWRP application for climate service at regional-local scales

The CWRP has been coupled with detailed models of terrestrial hydrology, coastal ocean, crop growth, air quality, and recently expanding interactive water quality and ecosystem. As such, the CWRP has been designed for climate applications at regional-local scales, and can be used to translate GCM global climate simulations into regional-specific actionable information for local impacts. This can be done by nesting CWRP with selected (*e.g.*, NOAA, NASA) operational forecasts of seasonal-interannual climate anomalies, and CMIP (*e.g.*, NCAR, GFDL) projections of future decadal climate changes under a feasible range of emissions scenarios. The CWRP can be run at multiple nested grids finer than 30-km to resolve the synoptic, mesoscale and local processes that govern the climate and environmental anomalies and changes most relevant to end-users for decision making. In so doing, the CWRP will be able to integrate the global signals with regional characteristics into comprehensive information required for local impacts assessment. We can further constrain the CWRP by the advanced data assimilation to improve initialization and narrow uncertainty such that the final prediction will be the most reliable source for end-users. We anticipate that the CWRP ensemble of multiple alternative physics configurations, with optimal weights on individual members as constrained by their respective performance metrics against observations, will further increase the downscaling predictive skill over the driving GCM forecasts or projections with more reliable estimate of result uncertainty. The CWRP optimized physics ensemble downscaling approach will provide an unprecedented skill enhancement for predicting climate at regional-local scales.

## References

- Choi, H.I., 2006: 3-D volume averaged soil-moisture transport model: A scalable scheme for representing subgrid topographic control in land-atmosphere interactions. *Ph.D. Dissertation*, University of Illinois at Urbana-Champaign, 189 pp.
- Choi, H.I., P. Kumar, and X.-Z. Liang, 2007: Three-dimensional volume-averaged soil moisture transport model with a scalable parameterization of subgrid topographic variability. *Water Resour. Res.*, **43**, W04414, doi:10.1029/2006WR005134, 15pp.
- Choi, H.I., X.-Z. Liang, and P. Kumar, 2011: A conjunctive surface-subsurface flow representation for mesoscale land surface models. *Water Resour. Res.* (submitted).
- Choi, H.I., and X.-Z. Liang, 2010: Improved terrestrial hydrologic representation in mesoscale land surface models. *J. Hydrometeorology*, **11**, 797–809.
- Dai, Y., R.E. Dickinson, and Y.-P. Wang, 2004: A two-big-leaf model for canopy temperature, photosynthesis, and stomatal conductance. *J. Climate*, **17**, 2281–2299.
- Dai, Y., X. Zeng, R.E. Dickinson, I. Baker, G.B. Bonan, M.G. Bosilovich, A.S. Denning, P.A. Dirmeyer, P.R. Houser, G. Niu, K.W. Oleson, C.A. Schlosser, and Z.-L. Yang, 2003: The Common Land Model. *Bull. Amer. Meteor. Soc.*, **84**, 1013–1023.
- Krishnamurti, T. N., C. M. Kishtawal, T. E. LaRow, D. R. Bachiochi, Z. Zhang, C. E. Williford, S. Gadgil, and S. Surendran, 1999: Improved weather and seasonal climate forecasts from multimodel superensemble. *Science*, **285**, 1548–1550.
- Liang, X.-Z., H. Choi, K.E. Kunkel, Y. Dai, E. Joseph, J.X.L. Wang, and P. Kumar, 2005a: Development of the regional climate-weather research and forecasting model (CWRf): Surface boundary conditions. *Illinois State Water Survey Scientific Research*, ISWS SR 2005-01, 32 pp. (<http://www.sws.uiuc.edu/pubs/pubdetail.asp?CallNumber=ISWS+SR+2005%2D01>).
- Liang, X.-Z., H. Choi, K.E. Kunkel, Y. Dai, E. Joseph, J.X.L. Wang, and P. Kumar, 2005b: Surface boundary conditions for mesoscale regional climate models. *Earth Interactions*, **9**, 1–28.
- Liang, X.-Z., L. Li, A. Dai, and K.E. Kunkel, 2004a: Regional climate model simulation of summer precipitation diurnal cycle over the United States. *Geophys. Res. Lett.*, **31**, L24208, doi:10.1029/2004GL021054.
- Liang, X.-Z., L. Li, K.E. Kunkel, M. Ting, and J.X.L. Wang, 2004b: Regional climate model simulation of U.S. precipitation during 1982–2002. Part 1: Annual cycle. *J. Climate*, **17**, 3510–3528.
- Liang, X.-Z., M. Xu, W. Gao, K.E. Kunkel, J. Slusser, Y. Dai, Q. Min, P.R. Houser, M. Rodell, C.B. Schaaf, and F. Gao, 2005c: Development of land surface albedo parameterization bases on Moderate Resolution Imaging Spectroradiometer (MODIS) data. *J. Geophys. Res.*, **110**, D11107, doi:10.1029/2004JD005579.
- Liang, X.-Z., M. Xu, K.E. Kunkel, G.A. Grell, and J. Kain, 2007: Regional climate model simulation of U.S.-Mexico summer precipitation using the optimal ensemble of two cumulus parameterizations. *J. Climate*, **20**, 5201–5207.
- Liang, X.-Z., M. Xu, X. Yuan, T. Ling, H.I. Choi, F. Zhang, L. Chen, S. Liu, S. Su, F. Qiao, J.X.L. Wang, K.E. Kunkel, W. Gao, E. Joseph, V. Morris, T.-W. Yu, J. Dudhia, and J. Michalakes, 2011: Regional Climate-Weather Research and Forecasting Model (CWRf). *Bull. Amer. Meteor. Soc.* (submitted).
- Mapes, B.E., T.T. Warner, M. Xu, and D.J. Gochis, 2004: Comparison of cumulus parameterizations and entrainment using domain-mean wind divergence in a regional model. *J. Atmos. Sc.*, **61**, 1284–1295.
- Oleson, K. W., G.-Y. Niu, Z.-L. Yang, D. M. Lawrence, P. E. Thornton, P. J. Lawrence, R. Stöckli, R. E. Dickinson, G. B. Bonan, S. Levis, A. Dai and T. Qian, 2008: Improvements to the Community Land Model and their impact on the hydrological cycle. *J. Geophys. Res.*, **113**, G01021, doi:10.1029/2007JG000563.
- Palmer, T. N., A. Alessandri, U. Andersen, P. Cantelaube, M. Davey, P. Délecluse, M. Déqué, E. Díez, F. J. Doblas-Reyes, H. Feddersen, R. Graham, S. Gualdi, J.-F. Guérémy, R. Hagedorn, M. Hoshen, N. Keenlyside, M. Latif, A. Lazar, E. Maisonave, V. Marletto, A. P. Morse, B. Orfila, P. Rogel, J.-M.

- Terres, and M. C. Thomson, 2004: Development of a European multimodel ensemble system for seasonal-to-interannual prediction (DEMETER). *Bull. Amer. Meteorol. Soc.*, **85**, 853–872.
- Peng, P., A. Kumar, H. van den Dool, and A. G. Barnston, 2002: An analysis of multimodel ensemble predictions for seasonal climate anomalies. *J. Geophys. Res.*, **107**(D23), 4710, doi:10.1029/2002JD002712.
- Skamarock, W.C., J.B. Klemp, J. Dudhia, D.O. Gill, D.M. Barker, M.G. Duda, X.-Y. Huang, W. Wang, and J.G. Powers, 2008: *A Description of the Advanced Research WRF Version 3*. NCAR Technical Note, NCAR/TN-475+STR, 113 pp.
- Wang, B., J.-Y. Lee, I.-S. Kang, J. Shukla, C.-K. Park, A. Kumar, J. Schemm, S. Cocke, J.-S. Kug, J.-J. Luo, T. Zhou, B. Wang, X. Fu, W.-T. Yun, O. Alves, E.K. Jin, J. Kinter, B. Kirtman, T. Krishnamurti, N.C. Lau, W. Lau, P. Liu, P. Pegion, T. Rosati, S. Schubert, W. Stern, M. Suarez, and T. Yamagata, 2009: Advance and prospectus of seasonal prediction: assessment of the APCC/CliPAS 14-model ensemble retrospective seasonal prediction (1980–2004). *Clim. Dyn.*, **33**, doi: 10.1007/s00382-008-0460-0.
- Yuan, X., and X.-Z. Liang, 2011a: Evaluation of a Conjunctive Surface-Subsurface Process model (CSSP) over the contiguous U.S. at regional-local scales. *J. Hydrometeorol*, **12**, 579–599, doi:10.1175/2010JHM1302.1.
- Yuan, X., and X.-Z. Liang, 2011b: Improving cold season precipitation prediction by the nested CWRF-CFS system. *Geophys. Res. Lett.*, **38**, L02706, doi:10.1029/2010GL046104.

#### ABBREVIATIONS AND ACRONYMS

ACM	Asymmetric Convective Model
AER	Atmospheric and Environmental Research
ARL	NOAA Air Resource Laboratory
BEP	Building Environment Parameterization (multilevel urban model)
BMJ	Betts-Miller-Janjic cumulus parameterization
BouLac	Bougeault-Lacarrère PBL scheme
CAM	NCAR Community Atmosphere Model
CAR	CWRF Cloud-Aerosol-Radiation Ensemble Modeling System
CAWCR	Centre for Australia Weather and Climate Research
CCCMA	Canadian Centre for Climate Modeling and Analysis
CFS	NCEP Climate Forecast System
CLM3.5	Community Land Model version 3.5
CMM5	Climate Extension of the PSU/NCAR Mesoscale Model generation 5
CoLM	Common Land Model
CMIP	Coupled Model Intercomparison Project
CROP	Dynamic crop growth modeling system
CSSP	Conjunctive Surface-Subsurface Process model
CSU	Colorado State University
CWRF	Climate extension of the Weather Research and Forecasting model
ECP	Ensemble Cumulus Parameterization modified from G3
ENSO	El Niño-Southern Oscillation
ESSIC	Earth System Science Interdisciplinary Center, University of Maryland
ETS	Equitable Threat Score
FLG	Fu-Liou-Gu radiation transfer scheme
G3	Grell-3 ensemble cumulus parameterization
GCM	General Circulation Model
GD	Grell-Dvénényi ensemble cumulus parameterization
GFDL	Geophysical Fluid Dynamics Laboratory
GR	Grell cumulus parameterization
GSFC	NASA Goddard Space Flight Center
HIR	High Resolution PBL scheme

---

LBCs	Lateral Boundary Conditions
Lin	Lin et al. microphysics scheme
MISC	Miscellaneous (obsolete) radiation schemes
MIT	Massachusetts Institute of Technology
Morrison	Morrison et al. two-moment microphysics scheme
MYJ	Mellor-Yamada-Janjic PBL scheme
MYNN	Mellor-Yamada PBL scheme modified by Nakanishi-Niino
NASA	National Aeronautics and Space Administration
NCAR	National Center for Atmospheric Research
NCAS	NOAA Center for Atmospheric Sciences
NCEP	National Centers for Environmental Prediction
NKF	New Kain-Fritsch cumulus parameterization
NOAA	National Oceanic and Atmospheric Administration
NOAH	NCAR-NCEP unified land surface model
ORO	Module for orographic turbulence stress and gravity-wave drag
PBL	Planetary Boundary Layer
PX	Pleim-Xiu land surface model
QNSE	Quasi-Normal Scale Elimination PBL scheme
<i>RadExt</i>	CWRF module for external radiative conditions (solar constant, atmospheric gas volume mixing ratios, aerosol distributions)
RCM	Regional Climate Model
RMSE	Root Mean Square Errors
SAS	Simplified Arakawa-Schubert cumulus parameterization
SBCs	Surface Boundary Conditions
<i>SfcExt</i>	CWRF module for external surface and subsurface conditions
SOM	Simple Ocean Model
SST	Sea Surface Temperature
Tao	Tao et al. microphysics scheme
TEMF	Total Energy–Mass Flux boundary layer scheme (Angevine et al. 2010)
Thompson	Thompson et al. microphysics scheme
UCM	Urban Canopy Model
UOM	Multilevel Upper Ocean Model
UW	University of Washington
WDM6	WRF Double-Moment 6-class microphysics scheme
WSM5	WRF Single-Moment 5-class microphysics scheme
WSM6	WRF Single-Moment 6-class microphysics scheme
WRF	Weather Research and Forecasting model
YSU	Yonsei University
ZML	Zhang-McFarlane-Liang cumulus parameterization